An Optimal Eigenvalue-Based Decomposition Approach for Estimating Forest Parameters Over Forest Mountain Areas

Nguyen Ngoc Tan and Minh Nghia Pham(✉)

Faculty of Radio-Electronics, Le Quy Don Technical University, Hanoi, Vietnam
nghiapm2018@mta.edu.vn

Abstract. This paper aims to provide a new method for retrieving forest parameters in forest mountain areas by using L-band polarimetric interferometry synthetic aperture radar (PolInSAR) data. Applying the model-based (ground, double-bounce, and volume scattering) decomposition techniques to PolInSAR data has opened a new way for vegetation parameters estimation. However, the modeling of the vegetation backscattering mechanisms is complicated due to the influences of the topographic slope variation and assumptions about the volume scattering component. In order to overcome these limitations, an eigenvalue-based decomposition technique is proposed. In which, a simple volume scattering model introduced by Neumann is used. The proposed method has improved 1.2664 m height of forest trees compared to the three-state inverse approach. In addition, evaluation results with simulated data generated from PolSARProSim software and PolInSAR data over the Kalimantan areas, Indonesia from ALOS/PALSAR L-band spaceborne radar system show that the proposed method produces reasonable and outstanding physical results in comparison with traditional decomposition methods.

Keywords: Polarimetric interferometry synthetic aperture radar · Forest height estimation · Coherence matrix · Three-stage

1 Introduction

Applying the model-based decomposition to polarimetric interferometry synthetic aperture radar (PolInSAR) data is an effective approach to separate scattering mechanisms in the natural environment. In recent years, this method has been widely applied to target detection and estimation of vegetation parameters. In general, model-based decomposition techniques are to accommodate a number of simple physical scattering models. The commonly applied decomposition techniques are mainly divided into two categories: (1) coherence decomposition based on the measured Sinclair matrix; (2) incoherent decomposition based on the measured coherency and covariance matrix [1–4]. In which, the three component decomposition of Freeman – Durden [5] is one of the most popular ones. Accordingly, the cross-correlation PolInSAR matrix obtained from observations can be described as the sum of three scattering sub-matrices, each representing the contributions of volume, ground, and double bounce scattering component. However, some major

N.-S. Vo and V.-P. Hoang (Eds.): INISCOM 2020, LNICST 334, pp. 221–232, 2020.
https://doi.org/10.1007/978-3-030-63083-6_17

shortcoming have been pointed out when applying this method, such as negative powers of ground scattering or double bounce scattering components and assumption of scattering reflection symmetry for volume scattering components. To effectively employed the Freeman–Durden decomposition algorithm, several assumptions are required for solving a nonlinear equation system. Recently, many modified methods have been proposed to overcome the mentioned shortcoming but mostly for modeling on relatively flat terrain and little research has been carried out on slope areas. On slope forest topography, local direction (OA) and local incidence angle are significantly changed by effect of slope terrain. This leads to a strong influence on the scattered signals. Therefore, scattering models in the Freeman – Durden decomposition are difficult to appropriately describe physical scattering mechanisms in sloping forest areas.

For these reasons, we proposed an eigenvalue-based decomposition approach for estimating forest parameters over forest mountain areas using single-baseline L-band PolInSAR data. In this approach, we shall suggest a simplified Neumann volume scattering model [6], which is characterized by a randomness parameter. This model is useful to overcome the limits of the scattering reflection symmetry assumption. This volume model includes both random and non-random volume situations, so it is suitable for volume scattering mechanisms on slope terrain. After that, the unknown parameters of the volume scattering matrix are determined as well as the parameters of the remain scattering mechanisms are estimated by using the optimal eigenvalue-based decomposition technique.

This paper is organized according to the following structure. In Sect. 2, basic scattering mechanisms and the simplified Neumann volume scattering model are introduced. Section 3 describes the optimal eigenvalue-based decomposition approach to estimate forest parameters. The estimated results by the proposed approach with simulated data and spaceborne data are given and discussed in Sect. 4. Finally, the conclusion and future work are presented in Sect. 5.

2 Basic Scattering Mechanisms in Forest Mountain Areas for PolInSAR and Simplified Neumann Volume Scattering Model

2.1 The PolInSAR Covariance Matrix

For PolInSAR, the obtained full polarimetric interferometry information data can be expressed in the form of two scattering matrices $[S_1]$ and $[S_2]$. The target vectors $\vec{k}_{L_1}$ and $\vec{k}_{L_2}$ in the lexicographic basis are measured at two ends of the baseline, as [7]

$$\vec{k}_{L_1} = [S_{1HH}, S_{1HV}, S_{1VV}]^T, \ \vec{k}_{L_2} = [S_{2HH}, S_{2HV}, S_{2VV}]^T \tag{1}$$

Accordingly, we can form the PolInSAR covariance matrix by multiplying the target vectors by their conjugate transpose

$$[T] = \left\langle \vec{k}\vec{k}^T \right\rangle = \begin{bmatrix} T_1 & \Omega \\ \Omega^T & T_2 \end{bmatrix} \text{ with } \vec{k} = \begin{bmatrix} \vec{k}_{L_1} \\ \vec{k}_{L_2} \end{bmatrix} \tag{2}$$

where $\langle . \rangle$ indicates the ensemble average in the data processing, the superscript $(.)^T$ denotes the complex conjugation. $[T_1]$ and $[T_2]$ are the normal Hermitian polarimetric covariance matrices for the two apertures, while $[\Omega]$ is a non- Hermitian cross-covariance matrix between the apertures and it contains both polarimetric information and interferometric information. As proposed in [8] and [9], the matrix $[\Omega]$ can be decomposed into three sub-matrices $[T_v]$, $[T_d]$ and $\left[T_g\right]$ which correspond to the volume, double bounce, and ground scattering mechanisms, respectively.

$$[\Omega] = e^{j\phi_g} f_v [T_v] + e^{j\phi_d} f_d [T_d] + e^{j\phi_v} f_g \left[T_g\right] \tag{3}$$

where f_v, f_d, f_g correspond to the contribution of the volume, double-bounce, ground scattering and ϕ_v, ϕ_d, ϕ_g are the phases of the three scattering components.

2.2 Volume Scattering Mechanism and Simplified Neumann Scattering Model

As suggested in [9, 10], the scattering from a tree canopy can be logically described by a multitude of randomly oriented particles. For each single particle, the normalized coherency matrix can be expressed as

$$T_\delta = \begin{bmatrix} 1 & \delta & 0 \\ \delta^* & |\delta|^2 & 0 \\ 0 & 0 & 0 \end{bmatrix} \tag{4}$$

with δ is the scattering anisotropy. When $|\delta|$ changes from 0 to 1, that mean the shape of particle varies from an isotropic sphere to a dipole, respectively. Neumann *et al.* [11] proposed the von Misses distribution for the orientation of particles. Accordingly, the coherency matrix is transformed as follows

$$T_v(\delta, \tau) = \begin{cases} \dfrac{1}{1+|\delta|^2} \begin{bmatrix} 1 & (1-\tau)\delta & 0 \\ (1-\tau)\delta^* & (1-\tau)|\delta|^2 & 0 \\ 0 & 0 & \tau|\delta|^2 \end{bmatrix} & \tau \le \dfrac{1}{2} \\ \dfrac{1}{1+|\delta|^2} \begin{bmatrix} 1 & (1-\tau)\delta & 0 \\ (1-\tau)\delta^* & |\delta|^2/2 & 0 \\ 0 & 0 & |\delta|^2/2 \end{bmatrix} & \tau > \dfrac{1}{2} \end{cases} \tag{5}$$

with $\tau \in [0, 1]$ denotes the normalized degree of orientation randomness.

Assume that forest areas consist mainly of dipoles ($\delta = \pm 1$) [12], the two coherency matrix are obtained as follows

$$T_v^H = \begin{cases} \dfrac{1}{2} \begin{bmatrix} 1 & 1-\tau & 0 \\ 1-\tau & 1-\tau & 0 \\ 0 & 0 & \tau \end{bmatrix} & \tau \le \dfrac{1}{2} \\ \dfrac{1}{2} \begin{bmatrix} 1 & 1-\tau & 0 \\ 1-\tau & 1/2 & 0 \\ 0 & 0 & 1/2 \end{bmatrix} & \tau > \dfrac{1}{2} \end{cases}; \; T_v^V = \begin{cases} \dfrac{1}{2} \begin{bmatrix} 1 & \tau-1 & 0 \\ \tau-1 & 1-\tau & 0 \\ 0 & 0 & \tau \end{bmatrix} & \tau \le \dfrac{1}{2} \\ \dfrac{1}{2} \begin{bmatrix} 1 & \tau-1 & 0 \\ \tau-1 & 1/2 & 0 \\ 0 & 0 & 1/2 \end{bmatrix} & \tau > \dfrac{1}{2} \end{cases} \tag{6}$$

where T_v^H and T_v^V are the horizontal and vertical simplified Neumann volume scattering models. In case $\tau = 1$ then $T_v^H = T_v^V$.

According to the analysis presented in [6], the copolarization power ratio $\gamma(\Omega) = \langle|S_{hh}|^2\rangle / \langle|S_{vv}|^2\rangle$ is capable of distinguishing the two types of the volume scattering model that shown in Eq. (6) and this ratio is highly correlated with the orientation randomness degree τ. We can derive $\gamma(\Omega)$ from cross-covariance matrix Ω and for each value of τ in the range [0, 1], the ratio $\gamma(T_v(\tau))$ can be obtained from the volume scattering matrix $T_v(\tau)$. Therefore, the optimum τ can be determined when the difference between these two ratios is minimal, i.e.,

$$\min|\gamma(\Omega) - \gamma(T_v(\tau))| \tag{7}$$

When τ is computed for each pixel, the corresponding volume scatterring matrix T_V is determined. Figure 1 shows an algorithm flowchart for determining the volume scattering matrix.

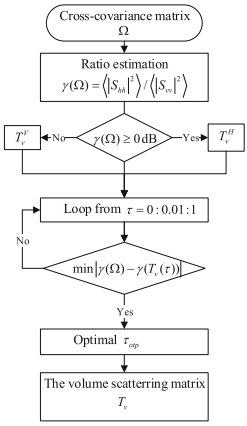

Fig. 1. Flowchart for determining volume scatter matrix

2.3 Ground and Double-Bounce Scattering Model for Sloped Terrain

For sloped terrain such as forest mountain areas, variations of topography and the local orientation angle due to the local terrain will lead to a change in the scattered signal. A local coordinate system is formed to accommodate the inclined ground surface. In order to represent the scattering components in the forest mountain areas, the flat double-bounce and ground scattering components are replaced by the scattering from the inclined ground plane [13]. In this case, the coherence scattering matrix for the ground and double-bounce contribution is created from the rotation of a local orientation angle χ represented as [14]

$$[T_d(\chi)] = \begin{bmatrix} |\alpha|^2 & \alpha\eta & 0 \\ \alpha^*\eta & \kappa & 0 \\ 0 & 0 & (1-\kappa) \end{bmatrix} \quad [T_g(\chi)] = \begin{bmatrix} 1 & \beta\eta & 0 \\ \beta^*\eta & |\beta|^2\kappa & 0 \\ 0 & 0 & |\beta|^2(1-\kappa) \end{bmatrix} \tag{8}$$

With $\kappa = \cos^2 2\chi p(\chi) d\chi$ and $\eta = \int \cos 2\chi p(\chi) d\chi$ denote the influence of terrain slope on the double-bounce and ground scattering mechanisms, respectively. The parameter κ is between 0.5 and 1 and η varies from 0 to 1 [11]. Two parameters α and β are the parameter of the double-bounce and ground scatterings as proposed by Freeman-Durden [5].

3 The Optimal Eigenvalue-Based Decomposition of PolInSAR Data

In this section, we propose an optimal eigenvalue-based decomposition approach for PolInSAR data to estimate vegetation parameters in mountain terrains. The approach is conducted in three steps. First, the terms of the volume scattering mechanism are identified. Next, an algorithm for analyzing the eigenvalue of the residual matrix is applied to determine the parameters of the ground and scattering mechanism. Finally, plant height is estimated by the canopy and ground phase difference.

From Eq. (3) and (8), we can transform as follows

$$\begin{aligned} [\Omega] - e^{j\phi_v} f_v [T_v] &= e^{j\phi_g} f_g \left[T_g\right] + e^{j\phi_d} f_d [T_d] \\ &= e^{j\phi_g} f_g \begin{bmatrix} 1 & \beta\eta & 0 \\ \beta^*\eta & |\beta|^2\kappa & 0 \\ 0 & 0 & |\beta|^2(1-\kappa) \end{bmatrix} + e^{j\phi_d} f_d \begin{bmatrix} |\alpha|^2 & \alpha\eta & 0 \\ \alpha^*\eta & \kappa & 0 \\ 0 & 0 & (1-\kappa) \end{bmatrix} \\ &= [\Omega_r] \end{aligned} \tag{9}$$

It is not difficult to recognize the unknown number identified as Eq. (10). To find the best fit forest parameters, $\left\{f_v, \phi_v, f_g, \phi_g, f_d, \phi_d, \alpha, \beta, \kappa, \eta\right\}$, the eigenvalues of two matrices $[\Omega_r]$ are determined by Eigen-decomposition techniques. Then, the eigenvalues are confined to zero, we can obtain canopy phase $\phi_v^i \{i = 1, 2, 3\}$ and the volume coefficients $f_v^i \{i = 1, 2, 3\}$

We assume that $\phi_v, f_v, \kappa, \eta$ are input loop parameters with $\kappa \in [0.5, 1]$ and $\eta \in [0, 1]$. For each value set $\{\phi_v, f_v, \kappa, \eta\}$ the residual matrix that contains the remaining two unknowns α, β can be obtained. We perform eigenvalue analysis for this residual matrix

$$[\Omega_r] = \lambda_1 \vec{k}_1 \vec{k}_1^* + \lambda_2 \vec{k}_2 \vec{k}_2^* \tag{10}$$

where λ_i and $\vec{k}_i = [u_{i1}, u_{i2}, u_{i3}]^T, (i = 1, 2)$ are eigenvalues and eigenvectors of residual matrix $[\Omega_r]$, respectively

We see that the minimum eigenvalue of the residual matrix is zero when the volume scattering component is completely removed from the PolInSAR data. As suggested by Cloude and Pottier [15], the parameter α is one of the main parameters for determining the dominant scattering component of independent targets. In this paper, we use an equivalent parameter μ_i to identify the dominant scattering mechanism. This parameter is determined as follows

$$\mu_i = \frac{|u_{i1}|}{\sqrt{|u_{i2}|^2 + |u_{i3}|^2}} \quad (i = 1, 2) \tag{11}$$

In case $\mu_i \geq 1$ for all i, the ground scattering component will be dominant and the parameters of the two scattering components are determined as follows

$$P_s = \lambda_1 + \lambda_2; \;\; P_d = 0; \;\; |\alpha| = \sqrt{\frac{P_s - \Omega_{r,11}}{\Omega_{r,11}}} \tag{12}$$

In case $\mu_i \leq 1$ for all i, the double-bounce scattering is the most dominant scattering and the parameters are determined in (13)

$$P_d = \lambda_1 + \lambda_2; \;\; P_s = 0; \;\; |\beta| = \sqrt{\frac{P_d - \Omega_{r,11}}{\Omega_{r,11}}} \tag{13}$$

On the contrary, if $\mu_i \geq 1$ and $\mu_j \leq 1$ $(i \neq j)$, both scattering components exist in the residual matrix $[\Omega_r]$, the parameters of the two scattering components are determined as follows

$$\alpha = \frac{u_{i1} + \sqrt{\lambda_r}\psi^{-1}u_{i3}e^{-j\zeta}}{u_{j1} + \sqrt{\lambda_r}\psi^{-1}u_{j3}e^{-j\zeta}}; \; \beta = \frac{u_{i1} - \sqrt{\lambda_r}\psi u_{i3}e^{-j\zeta}}{u_{j1} - \sqrt{\lambda_r}\psi^{-1}u_{j3}e^{-j\zeta}}; \; P_s = \lambda_i; \;\; P_d = \lambda_j; \;\; \lambda_r = \lambda_i/\lambda_j \tag{14}$$

The coefficients ψ and ζ are components of the identity matrix introduced by Yamaguchi [16]. Finally, the residual matrices are compared and the minimum residual matrix corresponds to the optimal parameter set. Based on the obtained parameters, the forest height can be estimated by the difference between canopy phase and surface phase, as in Eq. (15)

$$h_v = \frac{\phi_v - \phi_0}{k_z} \tag{15}$$

with ϕ_v, k_z are tree canopy phase, vertical wavenumber and ϕ_0 is surface phase obtained by using coherence set method [17].

The implementation steps of the proposed approach are summarized in Fig. 2.

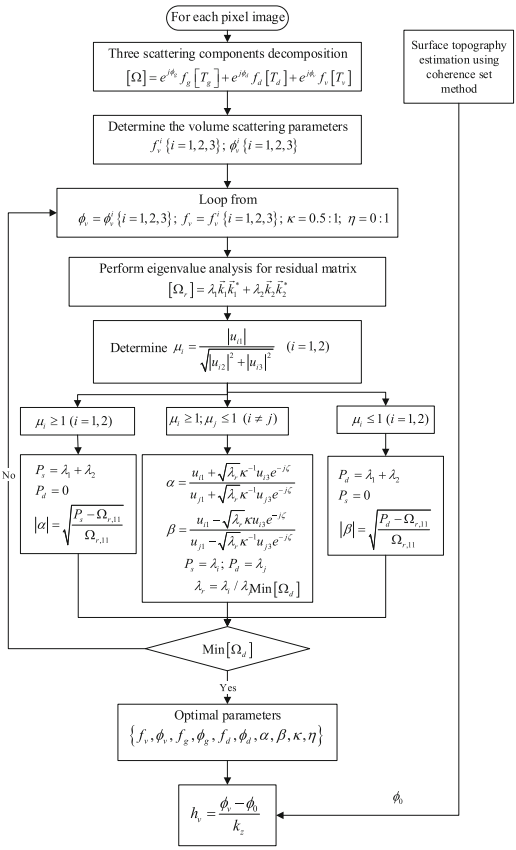

Fig. 2. Flowchart of the proposed approach

4 Applied Data Set and Experimental Results

To assess the effectiveness of the proposed method, a data set that is acquired from PolSARProSim software [18] is applied. The software performs data processing and it can generate simulated forest scenarios with similar parameters in actual scenarios. Accordingly, we created a forest scenario called HEDGE with an average tree height of 18 m. Forest area is 0.82745 Ha and tree density is 1000 stem/Ha. This is a sloped forest area with a slope in the azimuth of 16.7° (30%) and the slope in the direction of the range is 11.3° (20%). The interferometry polarimetric radar system is operated at frequency of 1.3 GHz and incidence angle of 45° when considering different soil conditions. The horizontal baseline is 15 m and the vertical baseline is 1.5 m. Azimuth resolution is 1.5 m whereas slant range resolution is 1 m.

The image of Pauli coded forest scenario is shown in Fig. 3 with an image size of 133 × 169 pixels in the range and azimuth direction, respectively. In this paper, we extract the results for analysis along the transect marked by the red line.

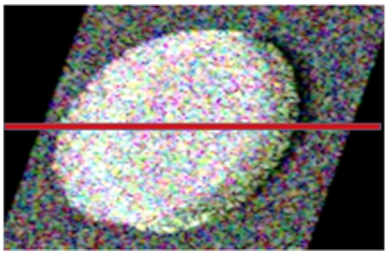

Fig. 3. Pauli coded forest image (Color figure online)

Figure 4 shows the tree forest height estimated by the optimal eigenvalue-based decomposition approach. The tree height obtained is completely consistent with it in a simulated scenario. In this picture, most peaks of the tree height are located at 18 m. At some pixels, tree height is estimated to be higher but still less than 22 m. Therefore, we can conclude that the estimated results from the proposed method are relatively accurate with small error rates.

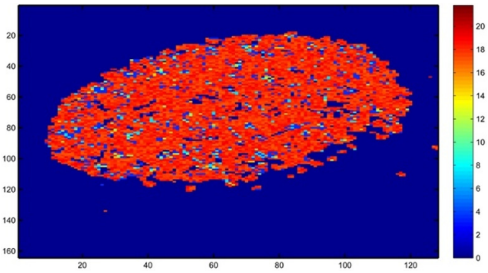

Fig. 4. The tree forest height estimated by the proposed approach

In order to further demonstrate the effectiveness of the optimal eigenvalue-based decomposition method, we implement comparing the results of the optimal eigenvalue-based decomposition approach with those obtained from the 3-stage inversion method [19]. This comparison is conducted in the 86^{th} row of the transect line. The results are detailed in Fig. 5 and Table 1.

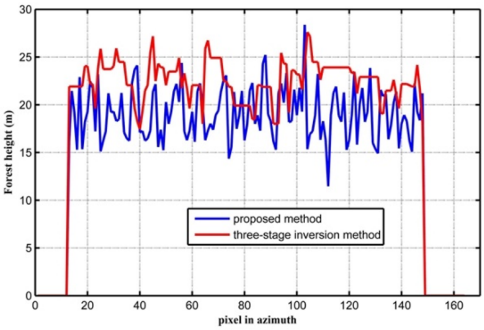

Fig. 5. The comparison of the results obtained from two methods

Table 1. The parameters are estimated by two methods

Parameter	Forest height h_v [m]	ϕ_v [rad]	Average errors [m]	RMSE (h_v) [m]
True	18	−0.157	0	0
Three - stage inversion	19.7325	−0.1218	1.5237	2.7052
Optimal eigenvalue-based decomposition method	17.5339	−0.1425	0.5788	2.5641

As mentioned in [19] by Cloude and Papathanassiou, the 3-stage algorithm performs forest height estimation by using a look-up table (LUT) to compare with the volume coherence. The accuracy of this algorithm depends on model predictions [19]. Therefore, the estimated results using this method are more inaccurate. Based on mathematical principles of eigenvalue analysis, the proposed method determined the optimal parameters for forest vegetation on sloped terrain. Therefore, the estimation results are significantly improved. This improvement is clearly shown by the parameters obtained in Fig. 6 and Table 1.

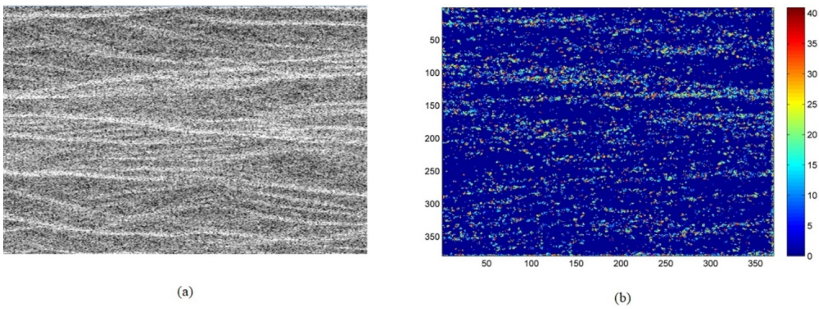

Fig. 6. The survey area: (a) HH polarized image and (b) the result of the proposed method

Next, we apply the proposed method to the satellite data set obtained from the ALOS system/PALSAR on March 12, 2007 for the first time and the second time on April 27, 2007. These include a pair of images of the jungle area at Kalimantan (1150 13′ 19″N, 1° 0′ 57″E), Indonesia. PolInSAR satellite system is operated at 1.3 Ghz frequency with baseline is 330 m and incidence angle is 21.5°. Figure 6a shows the HH polarized image of the survey area which is 375 × 384 pixels in size and the result of the proposed method is shown in Fig. 6b. This figure proves that most tree height on forest areas is approximately 20 m. Table 2 shows the detailed results in the forest parameter estimation using the proposed method for the survey area.

Table 2. Forest parameter estimation for survey area

Average height [m]	Fraction fill canopy r_h	RMSE (h_v) [m]	Volume phase [rad]
19.6942	0.4310	4.3976	0.0079

The amplitude of the ground, double-bounce and volume scattering mechanisms are shown in Fig. 7(a) and 7(b). For VV polarization channel, the volume scattering is the dominant component. For HH cross-correlation polarization channel, the contribution of the double-bound scattering component increased significantly. However, due to the slope of the terrain, this scattering mechanism is still not dominant in the vegetation areas and the contribution of volume scattering is still the largest. These results are completely consistent with the definition of Fresnel coefficients, in which the HH contribution exceeds the VV contribution.

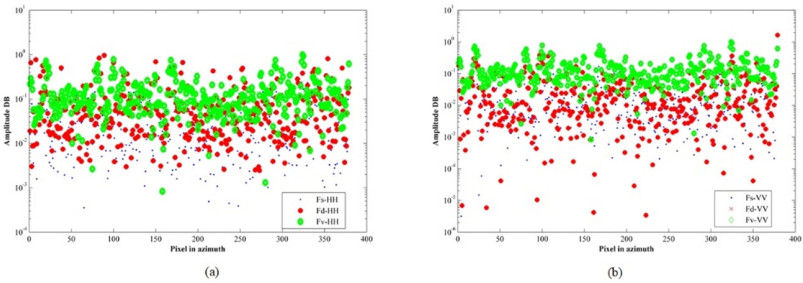

Fig. 7. Amplitude contributions of the three scattering mechanisms to the (a) HH, (b) VV polarized channel

5 Conclusion

A method for estimating vegetation parameters over forest mountain areas based on optimal eigenvalue-based decomposition technique has been proposed in this paper. The proposed decomposition method is implemented by introducing a simplified Neumann scattering model to fit the observed data on sloped terrain. Forest parameters were

obtained by the optimal eigenvalue analysis technique. In addition, scattering power and the contribution of scattering components are also estimated. Simulated data and experimental data from satellite system have been used to test this optimal eigenvalue algorithm. Obtained results indicated that vegetation parameters can be extracted directly and accurately. In the future, experiments will continue to be carried out on different terrains to more fully assess the effectiveness of the proposed method.

Acknowledgments. The research was funded by the Vietnam National Foundation for Science and Technology Development (NAFOSTED) under Grant No. 102.01-2017.04.

References

1. Cloude, S.R., Pottier, E.: A review of target decomposition theorems in radar polarimetry. IEEE Trans. Geosci. Remote Sens. **34**(2), 498–518 (1996)
2. Lee, J.-S., Pottier, E.: Polarimetric Radar Imaging, From Basics to Applications. CRC Press, Boca Raton (2009)
3. Cloude, S.: Polarisation Applications in Remote Sensing. Oxford University, London (2009)
4. Chen, S.-W., Li, Y.-Z., Wang, X.-S., Xiao, S.-P., Sato, M.: Modeling and interpretation of scattering mechanisms in polarimetric synthetic aperture radar: advances and perspectives. IEEE Signal Process. Mag. **31**(4), 79–89 (2014)
5. Freeman, A., Durden, S.L.: A three-component scattering model for polarimetric SAR data. IEEE Trans. Geosci. Remote Sens. **36**(3), 963–973 (1998)
6. Xie, Q., Zhu, J., Lopez-Sanchez, J.M., Wang, C., Fu, H.: A modified general polarimetric model-based decomposition method with the simplified Neumann volume scattering model. IEEE Geosci. Remote Sens. Lett. **15**, 1229–1233 (2018)
7. Boerner, W.M., Mott, H., Luneburg, E.: Polarimetry in radar remote sensing: basic and applied concepts. In: Henderson, F.M., Lewis, A.J. (eds.) Manual of Remote Sensing: Principles and Applications of Imaging Radar, New York, NY, USA, vol. 2 (1998)
8. Chen, S.W., Wang, X.S., Xiao, S.P., Sato, M.: General polarimetric model-based decomposition for coherency matrix. IEEE Trans. Geosci. Remote Sens. **52**(3), 1843–1855 (2014)
9. Xie, Q., Ballester-Berman, J.D., Lopez-Sanchez, J.M., Zhu, J., Wang, C.: On the use of generalized volume scattering models for the improvement of general polarimetric model-based decomposition. Remote Sens. **9**(2), 117 (2017)
10. Neumann, M.: Remote sensing of vegetation using multi-baseline polarimetric SAR interferometry: Theoretical modeling and physical parameter retrieval. Ph.D. dissertation, Institute of Electronics and Telecommunications of Rennes, Rennes University, Rennes, France, vol. 1 (January 2009)
11. Neumann, M., Ferro-Famil, L., Reigber, A.: Estimation of forest structure, ground, and canopy layer characteristics from multibaseline polarimetric interferometric SAR data. IEEE Trans. Geosci. Remote Sens. **48**(3), 1086–1104 (2010)
12. Antropov, O., Rauste, Y., Hame, T.: Volume scattering modeling in PolSAR decompositions: Study of ALOS PALSAR data over boreal forest. IEEE Trans. Geosci. Remote Sens. **49**(10), 3838–3848 (2011)
13. Park, S., Moon, W., Pottier, E.: Assessment of scattering mechanism of polarimetric SAR signal from mountain forest areas. IEEE Trans. Geosci. Remote Sens. **50**, 4711–4719 (2012)
14. Hajnsek, I., Pottier, E., Cloude, S.R.: Inversion of surface parameters from polarimetric SAR. IEEE Trans. Geosci. Remote Sens. **41**(7), 727–744 (2003)

15. Cloude, S.R., Pottier, E.: An entropy based classification scheme for land application of polarimetric SAR. IEEE Trans. Geosci. Remote Sens. **35**(1), 68–78 (1997)
16. Yamada, H., Yamazaki, M., Yamaguchi, Y.: On scattering model decomposition of PolSAR and its application to ESPRIT-based PolInSAR. In: Proceeding of 6th European Conference on Synthetic Aperture Radar, Dresden, Germany (May 2006)
17. Zou, B., Lu, D., Cai, H., Zhang, Y.: Ground topography estimation over forests using PolInSar image by means of coherence set. In: 18th IEEE International Conference Image Processing (ICIP) (2011)
18. Williams, M.L.: PolSARproSim: a coherent, polarimetric SAR simulation of forest for PolSARPro (2006). http://earth.eo.esa.int/polsarpro/SimulatedDataSources.html
19. Cloude, S.R., Papathanassiou, K.P.: Three-stage inversion process for polarimetric SAR interferometric. IEEE Proc. Radar Sonar Navig. **150**(3), 125–134 (2003)